HHS Public Access

Author manuscript

Neuron. Author manuscript; available in PMC 2017 June 15.

Published in final edited form as:

Neuron. 2016 June 15; 90(6): 1203–1214. doi:10.1016/j.neuron.2016.04.044.

Experience-Dependent Bimodal Plasticity of Inhibitory Neurons in Early Development

Hai-yan He[1], **Wanhua Shen**[2], **Masaki Hiramoto**[1], and **Hollis T. Cline**[1,*]

[1]The Dorris Neuroscience Center, Department of Molecular and Cellular Neuroscience, The Scripps Research Institute, 10550 North Torrey Pines Road, La Jolla, CA 92037, USA

[2]Key Lab of Organ Development and Regeneration of Zhejiang Province, College of Life and Environmental Sciences, Hangzhou Normal University, Hangzhou, Zhejiang 310036, China

Abstract

Inhibitory neurons are heterogeneous in the mature brain. It is unclear when and how inhibitory neurons express distinct structural and functional profiles. Using in vivo time-lapse imaging of tectal neuron structure and visually-evoked Ca^{++} responses in tadpoles we found that inhibitory neurons cluster into two groups with opposite valence of plasticity after 4h of dark and visual stimulation. Half decreased dendritic arbor size and Ca^{++} responses after dark and increased them after visual stimulation, matching plasticity in excitatory neurons. Half increased dendrite arbor size and Ca^{++} responses following dark and decreased them after stimulation. At the circuit level, visually-evoked excitatory and inhibitory synaptic inputs were potentiated by visual experience and E/I remained constant. Our results indicate that developing inhibitory neurons fall into distinct functional groups with opposite experience-dependent plasticity and as such, are well positioned to foster experience-dependent synaptic plasticity and maintain circuit stability during labile periods of circuit development.

eTOC blurb

Inhibitory tectal neurons demonstrate bimodal experience-dependent plasticity at early developmental stages, before establishment of classical biochemical and electrophysiological signatures of inhibitory neuronal subtypes. E/I balance is maintained following enhanced visual experience, through opposite plasticity responses of inhibitory neuronal subgroups.

* cline@scripps.edu.

Author Contributions

H-Y.H. and H.T.C. conceived and designed the project. H-Y.H. performed the structural and functional imaging experiments and analyzed the data. W.S. performed the in vivo patch clamp recordings and analyzed the data. M.H. built the in vivo functional imaging apparatus. H-Y.H. and H.T.C wrote the manuscript.

Introduction

GABAergic inhibition plays key roles during circuit development, such as controlling development of receptive field properties, modulating the gain, timing and firing of excitatory neurons, and gating critical periods for plasticity (Carvalho and Buonomano, 2009; Gabernet et al., 2005; Hensch et al., 1998; Huang et al., 1999; Kirkwood and Bear, 1995; Pouille et al., 2009; Pouille and Scanziani, 2001; Richards et al., 2010; Shen et al., 2011; Tao and Poo, 2005). In mature circuits, GABAergic inhibitory neurons are known for their structural and functional heterogeneity (Petilla Interneuron Nomenclature et al., 2008). Emerging evidence demonstrates that different types of inhibitory neurons exhibit distinct plastic changes in response to experience or activity (Bartley et al., 2008; Chen et al., 2015; Wolff et al., 2014). Even though the fate of GABAergic inhibitory neurons is thought to be determined during embryonic stages of development (Batista-Brito et al., 2008), the biochemical, morphological and electrophysiological features of different types are not fully established until postnatal development (Anastasiades et al., 2016; Batista-Brito and Fishell, 2009; Kuhlman et al., 2011). While it is known that the development of many aspects of GABAergic inhibition is influenced by experience and activity (Chattopadhyaya et al., 2004; Dobie and Craig, 2011; Jiao et al., 2006; Keck et al., 2011; Kreczko et al., 2009; Kuhlman et al., 2011; Maffei et al., 2006; Marik et al., 2010; Micheva and Beaulieu, 1995; Morales et al., 2002; Schuemann et al., 2013), it is unclear when and how developing inhibitory neurons exhibit distinct structural and functional profiles or whether experience-dependent plasticity profiles may help distinguish different types of inhibitory neurons at early stages of circuit development. To address this question we studied the structural and functional plasticity of optic tectal neurons in response to visual experience in Xenopus tadpoles. Inhibitory and excitatory neurons in the optic tectum are generated in a common proliferative zone and integrate into the optic tectal circuit at the same time (Akerman and Cline, 2006; Muldal et al., 2014). About 30% of optic tectal neurons are GABA-immunoreactive (Antal, 1991; Miraucourt et al., 2012), comparable to other brain regions and species (Caputi et al., 2013). Prior work has shown that visual experience promotes the structural and functional development of tectal neurons and the connectivity required for visual information processing (Ruthazer and Aizenman, 2010). These studies were conducted by randomly sampling tectal neurons without knowledge of neurotransmitter phenotype, and therefore likely reflect changes in the majority excitatory neuron population. Little is known about inhibitory neurons in the developing tectum, except that GABA is hyperpolarizing in the tadpole stages studied here (Akerman and Cline, 2006; Tao and Poo, 2005) and visual experience increases GABA levels (Miraucourt et al., 2012), consistent with other reports (Hendry and Jones, 1988; Kreczko et al., 2009; Morales et al., 2002; Sarro et al., 2008). In addition, electrophysiological recordings indicate that tectal neurons do not yet display characteristic features of mature inhibitory neurons, such as fast spiking, at these developmental stages (Ciarleglio et al., 2015). These studies suggest that the developing optic tectum provides an opportunity to investigate the development of structural and functional heterogeneity in inhibitory neurons.

Here we investigated structural and functional plasticity of inhibitory neurons in reference to excitatory neurons after periods of decreased and enhanced visual experience. Time-lapse

images of complete dendritic arbor structure and visually evoked Ca^{++} responses in single neurons were collected from animals exposed to 4h dark followed by 4h of short term visual enhancement (STVE) as measures of neuronal input and output, respectively. We found that although inhibitory neurons do not yet express calcium binding proteins that distinguish different types of inhibitory neurons at later developmental stages, they cluster into two groups that display opposite experience-dependent structural and functional plasticity. At the circuit level, in vivo whole cell recordings showed that enhanced visual experience potentiated both excitatory and inhibitory inputs to tectal neurons, so the balance of excitatory and inhibitory inputs (E/I) was maintained, consistent with the idea that the two inhibitory neuron groups may function in an indirect disinhibitory circuit. These results suggest that functionally distinct subpopulations of inhibitory tectal neurons emerge before the full expression of cell-type specific reporter proteins, and these inhibitory neuron subpopulations may play diverse roles in experience-dependent plasticity and in stabilizing neuronal circuits in the face of a changing environment.

Results

Inhibitory and excitatory tectal neurons have similar dendritic arbor structure

To determine whether inhibitory and excitatory tectal neurons can be distinguished based on distinct dendritic arbor structure or their distribution in the tectum, we collected in vivo time-lapse images of GFP-expressing neurons at daily intervals over 3 days, followed by posthoc identification of inhibitory and excitatory neurons based on GABA immunolabeling (Miraucourt et al., 2012; Wu and Cline, 1998). We imaged tectal neurons 8-10 days after electroporating GFP-expressing constructs, when they were incorporated into the functional retinotectal circuit, and synaptic GABAergic currents are hyperpolarizing (Akerman and Cline, 2006). Images and dendritic reconstructions of representative inhibitory and excitatory neurons are shown in Figure 1A, B. Flattened projections (Figure 1C, D) and single optical sections of the GABA-immunolabeled optic tectum with the GFP-labeled neuron, demonstrate the workflow to identify the transmitter phenotype of the imaged neurons used throughout the study. Quantitative morphometric analysis of total dendritic branch length (TDBL) and total branch tip number (TBTN) of the reconstructed dendritic arbors showed no significant change in TDBL or TBTN in inhibitory and excitatory neurons over the 3-day imaging period (Figure 1E), indicating that their dendritic arbor growth had plateaued, in contrast to the rapid dendritic arbor growth in immature tectal neurons (Cline, 2001; Wu and Cline, 1998). Inhibitory neuron dendritic arbors (TDBL and TBTN) were smaller than excitatory neurons on the third day of imaging (Figure 1E, Inset), consistent with Sholl analysis of day 3 data showing that inhibitory neurons are more sparsely branched than excitatory neurons (Figure 1F). The spread of individual data points (Figure 1E, right), together with the overlapping distribution of excitatory and inhibitory neurons in the tectum (Figure 1G) suggest that neither gross dendritic morphology (Figure 1H, I) nor soma location are sufficient to distinguish individual inhibitory and excitatory neurons.

Bimodal experience-dependent structural plasticity in inhibitory neurons

To study if inhibitory neurons exhibit experience-dependent structural plasticity and how it compares to that of excitatory neurons, animals were exposed to 4hr dark followed by 4hr

STVE. Individual neurons were imaged before and after each 4hr period (Figure 2A). Serial section electron microscopy of tectal neurons demonstrates that the majority of dendritic branch tips have synapses (Li et al., 2011), so changes in branch tip number are a proxy for changes in the number of synaptic inputs, a kin to spine dynamics in mature pyramidal neurons (Holtmaat and Svoboda, 2009). Despite their overall stability in dendritic arbor structure, excitatory neurons significantly increased TDBL and TBTN over 4h in STVE compared to dark (Figure S1). By contrast, the inhibitory population showed no significant change in the median dendritic arbor size over 4h in STVE (Figure 2B). Plotting changes in TBTN in individual inhibitory neurons over dark versus STVE showed a remarkable inverse correlation between structural changes in response to STVE versus dark: neurons that decreased TBTN over 4h in the dark increased TBTN with subsequent STVE; neurons that increased TBTN over 4h in the dark then decreased TBTN with STVE (Figure 2C, $r=-0.76$, $p=8.6e^{-6}$, Pearson correlation).

To test whether these inversely correlated structural changes in response to dark/STVE depend on the sequence of stimuli, we presented animals with STVE/dark (Figure 2D). Excitatory neuronal dendritic arbor size increased significantly over STVE compared to the subsequent dark period (FigureS1A-D), whereas the population of inhibitory neurons showed no significant change in arbor size in STVE compared to dark (Figure 2E). Again, scatterplots of individual inhibitory neurons demonstrated the same inverse correlation between structural plasticity in STVE versus dark as seen in dark/STVE (Figure 2F, $r=-0.87$, $p=2.5e^{-4}$, Pearson correlation). Data from both protocols completely co-mingled when plotted together (Figure 2G), suggesting that the visual experience-dependent structural plasticity of individual inhibitory neurons in response to brief periods of dark and STVE was determined by the experience that the animal had just had rather than the order of stimuli. Furthermore, the strong inverse correlation between dendritic arbor growth and retraction to dark and STVE in individual neurons held true ($r=-0.784$, $p=9.50e^{-09}$, Pearson correlation).

Experience-dependent structural plasticity revealed two populations of inhibitory neurons

The population of inhibitory neurons appears to fall into two groups that counteract each other with respect to the valence of plasticity (Figure 2G). To better evaluate this, we applied unsupervised cluster analysis to the entire inhibitory neuron data set based on changes of TBTN in response to STVE versus dark. The inhibitory neurons clustered into two evenly-sized subpopulations (Group I: n=18; Group II: n=24, Figure 3A). Changes in TDBL displayed similar separation between Groups I and II, even though the cluster analysis was based solely on TBTN data (Figure 3B). Neurons in the two groups displayed opposite signatures of experience-dependent structural plasticity. Group I neurons retracted dendrites in the dark and grew in STVE (similar to excitatory neurons; Figure S1). Group II neurons grew in the dark and retracted in STVE (Figure 3C). In either dark or STVE, structural changes in Group I and II canceled each other out, which explains the lack of net change in the total inhibitory population (Figure 2B).

To see if there is any regional bias in the distributions of Group I and Group II inhibitory neurons, we mapped the soma location of each imaged neuron onto a standard tectal profile.

Group I and II inhibitory neurons were similarly distributed throughout the tectum (Figure 3D). To examine if the two groups of inhibitory neurons belong to neuronal subtypes that can be characterized by the expression of different calcium-binding protein markers, we labeled optic tectal sections with antibodies to parvalbumin, somatostatin, calbindin, and calretinin, which label neurons in older animals (Gabriel et al., 1998; Laquerriere et al., 1989; Sanna et al., 1993; Stuesse et al., 2001). Most of these biochemical markers were either undetectable (calbindin), expressed at very low levels (parvalbumin, somatostatin), likely due to the relatively early developmental stages we studied compared to other studies, or labeled both inhibitory and excitatory neurons (calretinin; Figure S2). These data, together with the morphological analysis, suggest that tectal inhibitory neurons demonstrate functional heterogeneity before the establishment of biochemically or anatomically defined neuronal subtypes.

Opposite experience-dependent branch dynamics in Group I and Group II inhibitory neurons

The increased branch tip number we observed following STVE or dark could result from different cellular mechanisms, such as increased rate of branch additions or decreased rate of branch retractions, each associated with different mechanistic and functional implications (He and Cline, 2011). Likewise, decreased branch tip number could be due to decreased branch additions or increased branch retractions. With the power of time-lapse imaging, we resolved these possibilities by serial dynamic analysis of the dendritic structure of individual neurons. Figure 4A illustrates the analysis and categorization of branch dynamics. Fully reconstructed dendritic arbors of each neuron at sequential time points were aligned and compared in pairs to identify similar and different branches (Figure 4A, 4B). These data were then used to generate serial dynamic analysis results for each neuron (Figure 4A, B). Branches were categorized as stable, retracted, newly added and transient based on their presence at different time points, as illustrated (Figure 4A). Group I and II inhibitory neurons displayed opposite changes of branch tip dynamics following 4h in dark and STVE (Figure 4C). Group I inhibitory neurons had significantly more branch additions and fewer retractions in response to STVE compared to dark. Group II inhibitory neurons had significantly more additions and fewer retractions in the dark compared to STVE. Both branch retractions and additions contributed significantly to experience-dependent structural changes observed in either group of inhibitory neurons and seem to be coordinated so that whenever there are more retractions, additions decrease, and vice versa. As a result, the total number of dynamic branches (newly added plus retracted) did not differ in response to dark or STVE. Among all branches that retracted in response to STVE, some had been stable through the dark, and others were newly added during the dark (Figure 4A). We examined whether branches added during the dark were more prone to retraction in STVE than branches that persisted through the dark, and found that newly added branches were significantly more likely to be retracted with STVE than stable branches, suggesting that pre-existing branches are more persistent than the newly added ones (Figure 4D). Overall, the dynamic analysis demonstrated that Group I and Group II inhibitory neurons have fundamentally different responses to visual experience because dark or STVE induces opposite structural plasticity by controlling addition and pruning of branches.

Time-lapse functional imaging reveals bimodal visual experience-dependent plasticity in inhibitory neurons

The structural plasticity of dendritic arbors reported above indicates that inputs to tectal inhibitory and excitatory neurons are differently regulated by visual experience. To test whether there are corresponding experience-dependent changes in their outputs, we collected time-lapse images of visually-evoked somatic Ca^{++} responses in individual tectal neurons in awake animals exposed to the dark/STVE protocol. Visually-evoked somatic Ca^{++} responses are highly correlated with tectal cell firing (Niell and Smith, 2005; Podgorski et al., 2012; Xu et al., 2011). We imaged GCaMP6 signals in response to full field light on/off stimulation before and after 4h in dark and STVE and identified inhibitory neurons by posthoc GABA immunolabeling (Figure 5A). Both inhibitory and excitatory tectal cells responded to visual stimulation with Ca^{++} transients (Figure 5B, Figure S3A). STVE potentiated visually-evoked Ca^{++} responses in excitatory neurons, with no change following 4h in dark (Figure S3), similar to changes of dendritic arbor. In the total population of inhibitory neurons, neither the median Ca^{++} responses nor the median change in visually-evoked Ca^{++} responses over dark and STVE were different (Figure 5B, C). We again noted large variance in the changes in Ca^{++} responses over the 4h in dark and STVE. Scatterplots of changes in Ca^{++} after STVE versus dark in individual inhibitory neurons demonstrated a significant inverse correlation of functional plasticity following STVE versus dark (Pearson correlation, r=-0.76, $p < 0.0001$; Figure 5D), similar to the structural plasticity data. Neurons with potentiated visually-evoked Ca^{++} responses in STVE showed depressed Ca^{++} responses after dark, and neurons with potentiated Ca^{++} responses after dark showed depressed visually-evoked Ca^{++} responses after STVE. In addition, inhibitory neurons exhibited a significantly larger range of changes in Ca^{++} responses than excitatory neurons, especially after dark (Dark: $p<0.001$; STVE: $p<0.05$; two-sample F test, Figure 5E). The latency to the peak Ca^{++} responses decreased in both excitatory and inhibitory neurons following STVE (T_3 versus T_2, Figure 5F, Figure S3D), possibly reflecting increased response fidelity to potentiated retinotectal inputs following STVE (see Figure 8) (Song et al., 2000).

To control for variation in Ca^{++} responses across recording sessions, and to further test whether the changes in Ca^{++} responses were caused by the specific visual experience, we performed the same time-lapse functional imaging experiment in animals exposed to two consecutive 4h periods of ambient light (A1 and A2, Figure 5G, top). Neither excitatory nor inhibitory neurons showed significant differences in visually-evoked Ca^{++} responses before and after ambient light (Figure 5G, H, Figure S3E). There was no significant correlation of changes between the two ambient light sessions (Inhibitory neurons, Pearson correlation, r=0.353, p=0.18, Figure 5I; Excitatory neurons, Pearson correlation, r=0.046, p=0.8709; Figure S3F), nor a difference in the variance of changes in Ca^{++} peak amplitude between the inhibitory and excitatory neuronal populations following either ambient light period (A1: p=0.23, A2: p=0.12, two-sample F test, Figure 5J). Also, there was no change in the peak latency (Figure 5K, Figure S3F). This demonstrates that changes in visually-evoked Ca^{++} responses in the dark/STVE paradigm were induced by the specific visual experience.

Experience-dependent functional plasticity revealed two populations of inhibitory neurons

The Ca^{++} imaging data indicate that experience-dependent functional plasticity in inhibitory neurons is also bimodal. Unsupervised cluster analysis based on individual changes in Ca^{++} responses to STVE versus dark clustered the population into two groups (Group I: n=25; Group II: n=24; Figure 6A, B). Ca^{++} responses in Group I and II changed in opposite directions following dark and STVE (Figure 6C), strikingly similar to the Group I and Group II inhibitory neurons clustered by structural plasticity responses (Figure 3C). We named the two groups according to the valence of plasticity changes in response to dark and STVE, corresponding to the structural plasticity. These data, reflecting neuronal output, indicate that the inhibitory neuronal population consists of two functionally distinct groups that show plastic changes with opposite valence in response to the same visual experience. There was no difference in either the initial Ca^{++} amplitude or the peak latency between the two groups (Ca^{++} amplitude at T_1: Group I=1.88±0.47; Group II=1.07±0.28. peak latency at T_1 (sec): Group I=2.62±0.31; Group II=2.34±0.21. mean±SEM. $p>0.05$, Mann-Whitney U test), suggesting the two groups are not intrinsically different. On the other hand, cluster analysis of the inhibitory neuronal population exposed to sequential blocks of ambient light resulted in two uneven groups of 12 and 4 neurons (Figure 6D, E), and the responses of neurons within and between groups were not significantly different, supporting the idea that the distinct plasticity profiles observed in different groups of inhibitory neurons occur in response to specific visual experience (Figure 6F).

Structural and functional plasticity are correlated in individual tectal neurons

So far we have shown that tectal inhibitory neurons clustered into two groups based on the valence of structural and functional plasticity in response to visual experience. To test whether the valence of structural and functional plasticity is correlated in individual neurons, we collected time-lapse images of both the complete dendritic arbor and visually-evoked Ca^{++} responses in tectal neurons expressing tdTomato and GCaMP6. We examined the relationship between changes in TBTN and changes in the peak amplitude of Ca^{++} responses in individual neurons (regardless of their neural transmitter identity) before and after 4hr in dark followed by STVE or 4hr of STVE alone, as illustrated (Figure 7A). The valence of changes in TBTN and changes in peak Ca^{++} amplitude are correlated ($r=0.58$, $p < 0.05$, Pearson correlation, Figure 7B). Individual neurons that increased TBTN also increased visually-evoked Ca^{++} responses following the same visual experience. Similarly, experience that decreased TBTN decreased visually-evoked Ca^{++} responses in the same neuron, consistent with the idea that changes in dendritic arbor structure, reflecting neuronal input, correlate with changes in somatic Ca^{++} responses, reflecting functional output. Furthermore, overlaying the subset of data from inhibitory neurons in animals subjected to the dark/STVE protocol that we recorded in this experiment on the datasets from experiments described above shows that they also exhibit bi-modal structural and functional plasticity (Figure 7C, D). The relatively small magnitude of changes in GCaMP6 fluorescent in these neurons compared to the complete data set is likely due to the higher baseline fluorescence from the green emission of tdTomato. To our knowledge, this is the first in vivo demonstration of a direct correlation between structural changes in the complete dendritic arbor (total inputs) and functional changes in the outputs of individual neurons.

E/I is maintained after visual experience-dependent potentiation of retinotectal synaptic transmission

Many brain circuits maintain a balance between excitatory and inhibitory synaptic inputs onto postsynaptic neurons under various physiological conditions (Haider et al., 2006; Xue et al., 2014; Zhou et al., 2014). We have shown that disrupting E/I crippled Xenopus visual system function (Shen et al., 2011). Intuitively, maintaining E/I would require a tight correlation in plasticity in inhibitory and excitatory neuron populations. Our data indicate that there are two functionally distinct groups of inhibitory neurons in the optic tectum with opposite plasticity profiles, only one of which matches plasticity in excitatory neurons. How would these two counteracting inhibitory neuron groups affect E/I in the tectal circuit following enhanced visual experience? The effect of visual experience on E/I would likely depend on circuit connectivity between different types of neurons. Electrophysiological studies indicate that inhibitory tectal neurons receive direct retinal input and provide both feedforward inhibition to other retinorecipient neurons (Akerman and Cline, 2006) and feedback inhibition to regulate recurrent activity and visual information processing in the tectal circuit (Khakhalin et al., 2014; Pratt and Aizenman, 2007; Pratt et al., 2008). Immunoelectron microscopy showed that GABAergic inhibitory neurons receive both excitatory and GABAergic inputs, and they contact both inhibitory and excitatory neurons, providing evidence for both direct inhibitory circuits and indirect disinhibitory circuits in tectum (Rybicka and Udin, 1994). Figure 8A illustrates how visual experience might affect E/I in 3 possible circuit diagrams in which a postsynaptic tectal neuron (black) receives direct excitatory input (blue) and inputs from two groups of inhibitory neurons, configured for direct inhibitory or indirect disinhibitory circuits. In each circuit configuration, after STVE the excitatory input is potentiated. Depending on the connectivity of the two inhibitory neuron groups, the net inhibitory input to the postsynaptic neuron either remain unchanged, increase or decrease, which in turn results in either increased or unchanged E/I.

To determine which of these connectivity configurations is closer to the real situation, we tested the effect of STVE on E/I. We collected in vivo whole cell patch clamp recordings of visually-evoked synaptic currents from tectal neurons after animals received 4h of STVE or ambient light (Figure 8B, C). Both excitatory and inhibitory visually-evoked compound synaptic currents were potentiated by STVE (Figure 8D), and increased proportionally, so that E/I after STVE was similar to that in control animals (Figure 8E). Note that these observations are independent of the neurotransmitter identity of the recorded postsynaptic neuron. In addition, the excitatory and inhibitory synaptic inputs that we record are summed responses from all converging inputs, so inputs from specific types of neurons cannot be distinguished. These data support the idea that the two inhibitory neuron groups we observed are differentially involved in direct inhibitory and indirect disinhibitory circuits, consistent with the connectivity scheme in Figure 8Aiii, and further suggest that the bimodal experience-dependent plasticity of the Group I and II inhibitory neurons may be important in maintaining E/I following visual experience.

Discussion

Although it is widely recognized that neurons in mature sensory circuits exhibit cell type specific responses to sensory input, it is not clear when specific responses arise during initial stages of circuit development. Here we show, using unbiased sampling of neurons in the developing optic tectum, that there are two distinct groups of inhibitory neurons which display opposite structural and functional plasticity profiles in response to visual input even before they express classical biochemical markers characteristic of inhibitory neuronal cell types, and before tectal neurons exhibit distinct electrophysiological properties characteristic of mature inhibitory neurons (Ciarleglio et al., 2015) but when GABA is inhibitory (Akerman and Cline, 2006; Shen et al., 2011; Tao and Poo, 2005). The two functionally antagonizing inhibitory subpopulations may function through an indirect disinhibitory circuit and help to maintain the E/I balance in the circuit in response to changing experience.

Correlation of structural and functional plasticity

A basic tenet of neural plasticity is that experience-dependent changes in neuronal structure lead to changes in circuit function (Antonini et al., 1999; Cline, 2007; Katz and Shatz, 1996; Tropea et al., 2010). In vivo time-lapse imaging studies of cortical inhibitory neurons in adult mouse visual cortex have shown that monocular deprivation decreases synaptic inputs to layer 2/3 inhibitory neurons by increasing dendrite retraction and decreases neuronal output by decreasing axonal synaptic contacts with postsynaptic pyramidal cells (Chen et al., 2011). Additional studies identified layer- and neuron type-specific structural dynamics of inhibitory neurons in response to visual experience (Chen et al., 2012; Keck et al., 2011; Levelt and Hubener, 2012; van Versendaal et al., 2012). Together, these experiments indicate that experience-dependent structural changes in dendritic arbors reflect changes in neuronal input, and functional changes in output that translate into changes in circuit connectivity (Chen and Nedivi, 2010; Chklovskii et al., 2004; Cline and Haas, 2008). By evaluating both input (dendritic structure) and output (visually-evoked Ca^{++} transients), our study demonstrated that developing inhibitory neurons show bimodal plasticity in response to changes in visual experience and that two inhibitory neuronal groups can be identified based on their plasticity profiles. Furthermore, experiments in which we collected time-lapse structural and functional data from the same neurons in response to manipulating visual experience show that plasticity in the total dendritic arbor structure correlate with plasticity in visually-evoked Ca^{++} responses in individual neurons. These experiments suggest that the two groups of inhibitory neurons identified by structural plasticity correspond to the two groups identified by functional plasticity. They further provide a direct demonstration that structural changes in dendritic arbors and functional changes in neuronal output are correlated, for which previous studies on populations of neurons in several systems, including optic tectum, cerebellum and visual cortex had provided indirect evidence (Cline, 2007; McKay and Turner, 2005; Tropea et al., 2010). The correlation between plasticity of inputs and output of the neuron was observed regardless of the excitatory or inhibitory neurotransmitter identity of the neurons.

Bimodal visual-experience dependent plasticity in inhibitory neurons

Unlike most of other manipulations that involve deprivation or injury, we used a rather moderate experience manipulation (dark/STVE) in an effort to mimic the fluctuation of visual activity levels that animals might encounter in their daily environment. Our use of the dark/STVE protocol revealed several unusual features of inhibitory neuronal plasticity in response to visual experience. First, inhibitory neurons showed either positive or negative valence structural and functional plasticity to STVE, whereas excitatory neurons exhibited uniformly positive valence plasticity to the same visual experience. Second, the inhibitory neuronal population also showed bimodal structural and functional plasticity to dark, and the magnitude of plasticity in the dark was comparable to that induced by STVE, indicating that the lack of visual experience plays an active role in regulating the inhibitory neuronal response properties. Third, inhibitory neurons showed an inversely correlated bidirectional structural and functional plasticity to dark and STVE, such that inhibitory neurons that displayed positive valence plasticity to STVE showed a negative valence plasticity to dark, and vice versa. Finally, as a result of these bimodal responses, inhibitory neurons can be clustered into two subpopulations with opposite experience-dependent structural and functional plasticity profiles. The bimodal plasticity in response to dark and STVE is unique to inhibitory neurons, and was not seen in the excitatory neurons. Our study also draws attention to the critical information provided by longitudinal imaging studies of individual neurons. With population sampling, the distinct structural and functional plasticity that occurred in individual inhibitory neurons would be obscured.

Studies in adult mammalian brain indicate that different types of interneurons, identified by electrophysiological properties, expression of calcium-binding proteins, morphology, anatomical distribution, and lineage, play specific and diverse roles governing circuit activity (Basu et al., 2013; Gibson et al., 1999; Kepecs and Fishell, 2014; Kvitsiani et al., 2013; Royer et al., 2012; Wilson et al., 2012). Evidence that different types of inhibitory neurons undergo different forms of experience-dependent plasticity is also emerging. PV and SOM neurons show opposite plastic changes in fear conditioning (Wolff et al., 2014), and plasticity mechanisms of excitatory inputs to inhibitory neurons vary with the postsynaptic inhibitory cell types (Lu et al., 2007). Different classes of inhibitory neurons also play distinct roles in homeostatic plasticity: PV- and SOM-expressing neurons respond differently to prolonged TTX treatment in slice culture (Bartley et al., 2008). In mouse visual cortex, connections from layer 4 fast spiking neurons and regular spiking non-pyramidal neurons to pyramidal neurons undergo different visual deprivation induced homeostatic modifications (Maffei et al., 2004). Similarly, developmental auditory deprivation results in cell type- and pathway-specific homeostatic plasticity of inhibitory circuits (Takesian et al., 2010; Takesian et al., 2013). In agreement with these reports, we find two functionally distinct inhibitory neuron populations in the developing optic tectum, distinguished by their structural and functional plasticity responses to experience. In contrast to the above reports, however, the two groups of inhibitory neurons in our study could not be distinguished by biochemical markers, morphology or anatomical distribution. Our results indicate that inhibitory neurons operate within distinct circuits and play different functional roles in developing tectal circuits before the emergence of features of mature subtype.

Co-ordination of experience-dependent synaptic plasticity and E/I

Maintaining circuit stability by maintaining E/I and the generation of input-specific synaptic plasticity are thought to be required for the maturation and normal function of neural circuits. E/I is thought to remain relatively constant within individual neurons and across different brain activity states (Liu, 2004; Xue et al., 2014; Zhou et al., 2014). One paradox is that inhibition needs to decrease to allow potentiation of excitatory synapses, but inhibition should increase to balance increased excitation so that circuits remain stable. How do the two seemingly contradictory mechanisms work on the same circuitry elements and reconcile with each other? Our results suggest that one solution to this issue is to have subpopulations of inhibitory neurons which respond with opposite valence plasticity to dark and visual stimulation. Depending on the connectivity between excitatory and inhibitory neurons, such as feedforward or disinhibitory connections, the output of the microcircuit can be variable. Based on existing electrophysiological and anatomical evidence, we propose that these two groups of inhibitory neurons are differently involved in direct and indirect inhibitory pathways and work in concert to allow both synapse-specific refinement and E/I stability. It is also possible that these subgroups of inhibitory neurons target innervation to distinct subcellular compartments, as shown in frog tectum (Rybicka and Udin, 1994) and other systems (Basu et al., 2013; Huang et al., 2007). The plasticity we observed in response to the dark/STVE protocol may reveal mechanisms employed by circuits to maintain stability together with mechanisms underlying experience-dependent developmental maturation of neuronal response properties. Recent studies in mature circuits suggest that PV inhibitory neurons maintain E/I (Xue et al., 2014), whereas dendritically targeted SOM inhibitory neurons gate excitatory synaptic plasticity (Kvitsiani et al., 2013; Lovett-Barron et al., 2012; Wilson et al., 2012), and would therefore be expected to change in the opposite directions in reference to excitatory neurons to allow E/I stability and experience-dependent plasticity of specific excitatory synapses. Indeed a recent study in motor cortex indicates that structural plasticity in PV and SOM neurons do change in opposite directions with learning (Chen et al., 2015). These two circuit connectivity schemes are not mutually exclusive, as SOM neurons also innervate PV neurons (Letzkus et al., 2011; Pfeffer et al., 2013). Further investigation is needed to establish the exact connectivity pattern among excitatory and inhibitory tectal neurons.

Experimental Procedures

All animal protocols were approved by the Institutional Animal Care and Use Committee of the Scripps Research Institute.

In Vivo Time-Lapse Imaging of Dendritic Structure or Visually Evoked Ca^{2+} Responses

Tectal neurons were transfected with GFP or GCaMP6s (Chen et al., 2013) and imaged on a custom two-photon microscope with a 20x water immersion objective (Olympus XLUMPlanFL 0.95NA). Dendritic arbors were reconstructed using Imaris (Bitplane, US). Branch dynamic analysis was conducted with 4DSPA software (Lee et al., 2013). The peak amplitude of the Ca^{++} response to full field visual stimuli was calculated as percent change in fluorescence relative to the baseline fluorescence, measured over 1 second prior to the onset of the stimulus (dF/F_0).

To determine the variability of individual neuronal responses to visual stimuli, we recorded responses to 15-20 repeats of visual stimuli in a subset of neurons and used bootstrap to calculate the 95% confidence range of variation with any 5 repetitions was [−29%, 31%] of the mean value (Figure S4). To image the dendritic arbor and visually-evoked Ca^{++} responses in the same neuron, animals were co-electroporated with GCaMP6s and tdTomato constructs. In vivo patch clamp recording was conducted as described (Shen et al., 2011).

Cluster analysis and statistics

Cluster analysis was performed using an unsupervised agglomerative hierarchical tree method in MATLAB (linkage.m) based upon their pair-wise vectorial distance in the constructed 2D space (pdist.m). The threshold was arbitrarily set at the highest level that can separate the dataset into two clusters. See SOM for details of the choice of cluster analysis method and metrics (Table S1, Figure S5).

Nonparametric statistical analysis was performed in all statistical tests. Wilcoxon sign rank test was performed for within-cell comparison. Kruskal-Wallis test with posthoc Mann-Whitney U test were performed when comparing data across different groups of neurons with different visual experience.

See SOM for detailed information on experimental protocols.

Supplementary Material

Refer to Web version on PubMed Central for supplementary material.

Acknowledgements

We thank Dr. Hey-Kyoung Lee (Johns Hopkins University), Dr. Yi Zuo (University of California, Santa Cruz), Dr. Kurt Haas (University of British Columbia), Dr. Carlos Aizenman (Brown University) and members of Cline lab for critical comments and discussion on the manuscripts. This work was supported by a grant from the US National Institutes of Health (EY011261) and an endowment from the Hahn Family Foundation to HTC.

References

Akerman CJ, Cline HT. Depolarizing GABAergic conductances regulate the balance of excitation to inhibition in the developing retinotectal circuit in vivo. J Neurosci. 2006; 26:5117–5130. [PubMed: 16687503]

Anastasiades PG, Marques-Smith A, Lyngholm D, Lickiss T, Raffiq S, Katzel D, Miesenbock G, Butt SJ. GABAergic interneurons form transient layer-specific circuits in early postnatal neocortex. Nat Commun. 2016; 7:10584. [PubMed: 26843463]

Antal M. Distribution of GABA immunoreactivity in the optic tectum of the frog: a light and electron microscopic study. Neuroscience. 1991; 42:879–891. [PubMed: 1956520]

Antonini A, Fagiolini M, Stryker MP. Anatomical correlates of functional plasticity in mouse visual cortex. J Neurosci. 1999; 19:4388–4406. [PubMed: 10341241]

Bartley AF, Huang ZJ, Huber KM, Gibson JR. Differential activity-dependent, homeostatic plasticity of two neocortical inhibitory circuits. J Neurophysiol. 2008; 100:1983–1994. [PubMed: 18701752]

Basu J, Srinivas KV, Cheung SK, Taniguchi H, Huang ZJ, Siegelbaum SA. A cortico-hippocampal learning rule shapes inhibitory microcircuit activity to enhance hippocampal information flow. Neuron. 2013; 79:1208–1221. [PubMed: 24050406]

Batista-Brito R, Fishell G. The developmental integration of cortical interneurons into a functional network. Curr Top Dev Biol. 2009; 87:81–118. [PubMed: 19427517]

Batista-Brito R, Machold R, Klein C, Fishell G. Gene expression in cortical interneuron precursors is prescient of their mature function. Cereb Cortex. 2008; 18:2306–2317. [PubMed: 18250082]

Caputi A, Melzer S, Michael M, Monyer H. The long and short of GABAergic neurons. Curr Opin Neurobiol. 2013; 23:179–186. [PubMed: 23394773]

Carvalho TP, Buonomano DV. Differential effects of excitatory and inhibitory plasticity on synaptically driven neuronal input-output functions. Neuron. 2009; 61:774–785. [PubMed: 19285473]

Chattopadhyaya B, Di Cristo G, Higashiyama H, Knott GW, Kuhlman SJ, Welker E, Huang ZJ. Experience and activity-dependent maturation of perisomatic GABAergic innervation in primary visual cortex during a postnatal critical period. J Neurosci. 2004; 24:9598–9611. [PubMed: 15509747]

Chen JL, Lin WC, Cha JW, So PT, Kubota Y, Nedivi E. Structural basis for the role of inhibition in facilitating adult brain plasticity. Nat Neurosci. 2011; 14:587–594. [PubMed: 21478885]

Chen JL, Nedivi E. Neuronal structural remodeling: is it all about access? Curr Opin Neurobiol. 2010; 20:557–562. [PubMed: 20621466]

Chen JL, Villa KL, Cha JW, So PT, Kubota Y, Nedivi E. Clustered dynamics of inhibitory synapses and dendritic spines in the adult neocortex. Neuron. 2012; 74:361–373. [PubMed: 22542188]

Chen SX, Kim AN, Peters AJ, Komiyama T. Subtype-specific plasticity of inhibitory circuits in motor cortex during motor learning. Nat Neurosci. 2015; 18:1109–1115. [PubMed: 26098758]

Chen TW, Wardill TJ, Sun Y, Pulver SR, Renninger SL, Baohan A, Schreiter ER, Kerr RA, Orger MB, Jayaraman V, et al. Ultrasensitive fluorescent proteins for imaging neuronal activity. Nature. 2013; 499:295–300. [PubMed: 23868258]

Chklovskii DB, Mel BW, Svoboda K. Cortical rewiring and information storage. Nature. 2004; 431:782–788. [PubMed: 15483599]

Ciarleglio CM, Khakhalin AS, Wang AF, Constantino AC, Yip SP, Aizenman CD. Multivariate analysis of electrophysiological diversity of Xenopus visual neurons during development and plasticity. Elife. 2015; 4

Cline H, Haas K. The regulation of dendritic arbor development and plasticity by glutamatergic synaptic input: a review of the synaptotrophic hypothesis. J Physiol. 2008; 586:1509–1517. [PubMed: 18202093]

Cline HT. Dendritic arbor development and synaptogenesis. Curr Opin Neurobiol. 2001; 11:118–126. [PubMed: 11179881]

Cline, HT.; Santos Da Silva, J.; Bestman, J. Dendrite Development. Stuart, NSG.; Hausner, M., editors. Oxford University Press; London: 2007.

Dobie FA, Craig AM. Inhibitory synapse dynamics: coordinated presynaptic and postsynaptic mobility and the major contribution of recycled vesicles to new synapse formation. J Neurosci. 2011; 31:10481–10493. [PubMed: 21775594]

Gabernet L, Jadhav SP, Feldman DE, Carandini M, Scanziani M. Somatosensory integration controlled by dynamic thalamocortical feed-forward inhibition. Neuron. 2005; 48:315–327. [PubMed: 16242411]

Gabriel R, Volgyi B, Pollak E. Calretinin-immunoreactive elements in the retina and optic tectum of the frog, Rana esculenta. Brain Res. 1998; 782:53–62. [PubMed: 9519249]

Gibson JR, Beierlein M, Connors BW. Two networks of electrically coupled inhibitory neurons in neocortex. Nature. 1999; 402:75–79. [PubMed: 10573419]

Haider B, Duque A, Hasenstaub AR, McCormick DA. Neocortical network activity in vivo is generated through a dynamic balance of excitation and inhibition. J Neurosci. 2006; 26:4535–4545. [PubMed: 16641233]

He HY, Cline HT. Diadem X: automated 4 dimensional analysis of morphological data. Neuroinformatics. 2011; 9:107–112. [PubMed: 21271361]

Hendry SH, Jones EG. Activity-dependent regulation of GABA expression in the visual cortex of adult monkeys. Neuron. 1988; 1:701–712. [PubMed: 3272185]

Hensch TK, Fagiolini M, Mataga N, Stryker MP, Baekkeskov S, Kash SF. Local GABA circuit control of experience-dependent plasticity in developing visual cortex. Science. 1998; 282:1504–1508. [PubMed: 9822384]

Holtmaat A, Svoboda K. Experience-dependent structural synaptic plasticity in the mammalian brain. Nat Rev Neurosci. 2009; 10:647–658. [PubMed: 19693029]

Huang ZJ, Di Cristo G, Ango F. Development of GABA innervation in the cerebral and cerebellar cortices. Nat Rev Neurosci. 2007; 8:673–686. [PubMed: 17704810]

Huang ZJ, Kirkwood A, Pizzorusso T, Porciatti V, Morales B, Bear MF, Maffei L, Tonegawa S. BDNF regulates the maturation of inhibition and the critical period of plasticity in mouse visual cortex. Cell. 1999; 98:739–755. [PubMed: 10499792]

Jiao Y, Zhang C, Yanagawa Y, Sun QQ. Major effects of sensory experiences on the neocortical inhibitory circuits. J Neurosci. 2006; 26:8691–8701. [PubMed: 16928857]

Katz LC, Shatz CJ. Synaptic activity and the construction of cortical circuits. Science. 1996; 274:1133–1138. [PubMed: 8895456]

Keck T, Scheuss V, Jacobsen RI, Wierenga CJ, Eysel UT, Bonhoeffer T, Hubener M. Loss of sensory input causes rapid structural changes of inhibitory neurons in adult mouse visual cortex. Neuron. 2011:869–882. [PubMed: 21903080]

Kepecs A, Fishell G. Interneuron cell types are fit to function. Nature. 2014; 505:318–326. [PubMed: 24429630]

Khakhalin AS, Koren D, Gu J, Xu H, Aizenman CD. Excitation and inhibition in recurrent networks mediate collision avoidance in Xenopus tadpoles. Eur J Neurosci. 2014; 40:2948–2962. [PubMed: 24995793]

Kirkwood A, Bear MF. Elementary forms of synaptic plasticity in the visual cortex. Biol Res. 1995; 28:73–80. [PubMed: 8728822]

Kreczko A, Goel A, Song L, Lee HK. Visual deprivation decreases somatic GAD65 puncta number on layer 2/3 pyramidal neurons in mouse visual cortex. Neural Plast. 2009; 2009:415135. [PubMed: 19503840]

Kuhlman SJ, Tring E, Trachtenberg JT. Fast-spiking interneurons have an initial orientation bias that is lost with vision. Nat Neurosci. 2011; 14:1121–1123. [PubMed: 21750548]

Kvitsiani D, Ranade S, Hangya B, Taniguchi H, Huang JZ, Kepecs A. Distinct behavioural and network correlates of two interneuron types in prefrontal cortex. Nature. 2013; 498:363–366. [PubMed: 23708967]

Laquerriere A, Leroux P, Gonzalez BJ, Bodenant C, Benoit R, Vaudry H. Distribution of somatostatin receptors in the brain of the frog Rana ridibunda: correlation with the localization of somatostatin-containing neurons. The Journal of comparative neurology. 1989; 280:451–467. [PubMed: 2563740]

Lee PC, He HY, Lin CY, Ching YT, Cline HT. Computer aided alignment and quantitative 4D structural plasticity analysis of neurons. Neuroinformatics. 2013; 11:249–257. [PubMed: 23408326]

Letzkus JJ, Wolff SB, Meyer EM, Tovote P, Courtin J, Herry C, Luthi A. A disinhibitory microcircuit for associative fear learning in the auditory cortex. Nature. 2011; 480:331–335. [PubMed: 22158104]

Levelt CN, Hubener M. Critical-period plasticity in the visual cortex. Annu Rev Neurosci. 2012; 35:309–330. [PubMed: 22462544]

Li J, Erisir A, Cline H. In vivo time-lapse imaging and serial section electron microscopy reveal developmental synaptic rearrangements. Neuron. 2011; 69:273–286. [PubMed: 21262466]

Liu G. Local structural balance and functional interaction of excitatory and inhibitory synapses in hippocampal dendrites. Nat Neurosci. 2004; 7:373–379. [PubMed: 15004561]

Lovett-Barron M, Turi GF, Kaifosh P, Lee PH, Bolze F, Sun XH, Nicoud JF, Zemelman BV, Sternson SM, Losonczy A. Regulation of neuronal input transformations by tunable dendritic inhibition. Nat Neurosci. 2012; 15:423–430. S421–423. [PubMed: 22246433]

Lu JT, Li CY, Zhao JP, Poo MM, Zhang XH. Spike-timing-dependent plasticity of neocortical excitatory synapses on inhibitory interneurons depends on target cell type. J Neurosci. 2007; 27:9711–9720. [PubMed: 17804631]

Maffei A, Nataraj K, Nelson SB, Turrigiano GG. Potentiation of cortical inhibition by visual deprivation. Nature. 2006; 443:81–84. [PubMed: 16929304]

Maffei A, Nelson SB, Turrigiano GG. Selective reconfiguration of layer 4 visual cortical circuitry by visual deprivation. Nat Neurosci. 2004; 7:1353–1359. [PubMed: 15543139]

Marik SA, Yamahachi H, McManus JN, Szabo G, Gilbert CD. Axonal dynamics of excitatory and inhibitory neurons in somatosensory cortex. PLoS Biol. 2010; 8:e1000395. [PubMed: 20563307]

McKay BE, Turner RW. Physiological and morphological development of the rat cerebellar Purkinje cell. J Physiol. 2005; 567:829–850. [PubMed: 16002452]

Micheva KD, Beaulieu C. An anatomical substrate for experience-dependent plasticity of the rat barrel field cortex. Proc Natl Acad Sci U S A. 1995; 92:11834–11838. [PubMed: 8524859]

Miraucourt LS, Silva JS, Burgos K, Li J, Abe H, Ruthazer ES, Cline HT. GABA expression and regulation by sensory experience in the developing visual system. PLoS One. 2012; 7:e29086. [PubMed: 22242157]

Morales B, Choi SY, Kirkwood A. Dark rearing alters the development of GABAergic transmission in visual cortex. J Neurosci. 2002; 22:8084–8090. [PubMed: 12223562]

Muldal AM, Lillicrap TP, Richards BA, Akerman CJ. Clonal relationships impact neuronal tuning within a phylogenetically ancient vertebrate brain structure. Curr Biol. 2014; 24:1929–1933. [PubMed: 25127219]

Niell CM, Smith SJ. Functional imaging reveals rapid development of visual response properties in the zebrafish tectum. Neuron. 2005; 45:941–951. [PubMed: 15797554]

Petilla Interneuron Nomenclature G, Ascoli GA, Alonso-Nanclares L, Anderson SA, Barrionuevo G, Benavides-Piccione R, Burkhalter A, Buzsaki G, Cauli B, Defelipe J, et al. Petilla terminology: nomenclature of features of GABAergic interneurons of the cerebral cortex. Nat Rev Neurosci. 2008; 9:557–568. [PubMed: 18568015]

Pfeffer CK, Xue M, He M, Huang ZJ, Scanziani M. Inhibition of inhibition in visual cortex: the logic of connections between molecularly distinct interneurons. Nat Neurosci. 2013; 16:1068–1076. [PubMed: 23817549]

Podgorski K, Dunfield D, Haas K. Functional clustering drives encoding improvement in a developing brain network during awake visual learning. PLoS Biol. 2012; 10:e1001236. [PubMed: 22253571]

Pouille F, Marin-Burgin A, Adesnik H, Atallah BV, Scanziani M. Input normalization by global feedforward inhibition expands cortical dynamic range. Nat Neurosci. 2009; 12:1577–1585. [PubMed: 19881502]

Pouille F, Scanziani M. Enforcement of temporal fidelity in pyramidal cells by somatic feed-forward inhibition. Science. 2001; 293:1159–1163. [PubMed: 11498596]

Pratt KG, Aizenman CD. Homeostatic regulation of intrinsic excitability and synaptic transmission in a developing visual circuit. J Neurosci. 2007; 27:8268–8277. [PubMed: 17670973]

Pratt KG, Dong W, Aizenman CD. Development and spike timing-dependent plasticity of recurrent excitation in the Xenopus optic tectum. Nat Neurosci. 2008; 11:467–475. [PubMed: 18344990]

Richards BA, Voss OP, Akerman CJ. GABAergic circuits control stimulus-instructed receptive field development in the optic tectum. Nat Neurosci. 2010; 13:1098–1106. [PubMed: 20694002]

Royer S, Zemelman BV, Losonczy A, Kim J, Chance F, Magee JC, Buzsaki G. Control of timing, rate and bursts of hippocampal place cells by dendritic and somatic inhibition. Nat Neurosci. 2012; 15:769–775. [PubMed: 22446878]

Ruthazer ES, Aizenman CD. Learning to see: patterned visual activity and the development of visual function. Trends Neurosci. 2010; 33:183–192. [PubMed: 20153060]

Rybicka KK, Udin SB. Ultrastructure and GABA immunoreactivity in layers 8 and 9 of the optic tectum of Xenopus laevis. Eur J Neurosci. 1994; 6:1567–1582. [PubMed: 7850020]

Sanna PP, Keyser KT, Celio MR, Karten HJ, Bloom FE. Distribution of parvalbumin immunoreactivity in the vertebrate retina. Brain Res. 1993; 600:141–150. [PubMed: 8422581]

Sarro EC, Kotak VC, Sanes DH, Aoki C. Hearing loss alters the subcellular distribution of presynaptic GAD and postsynaptic GABAA receptors in the auditory cortex. Cereb Cortex. 2008; 18:2855–2867. [PubMed: 18403398]

Schuemann A, Klawiter A, Bonhoeffer T, Wierenga CJ. Structural plasticity of GABAergic axons is regulated by network activity and GABAA receptor activation. Frontiers in neural circuits. 2013; 7:113. [PubMed: 23805077]

Shen W, McKeown CR, Demas JA, Cline HT. Inhibition to excitation ratio regulates visual system responses and behavior in vivo. J Neurophysiol. 2011; 106:2285–2302. [PubMed: 21795628]

Song S, Miller KD, Abbott LF. Competitive Hebbian learning through spike-timing-dependent synaptic plasticity. Nat Neurosci. 2000; 3:919–926. [PubMed: 10966623]

Stuesse SL, Adli DS, Cruce WL. Immunohistochemical distribution of enkephalin, substance P, and somatostatin in the brainstem of the leopard frog, Rana pipiens. Microsc Res Tech. 2001; 54:229–245. [PubMed: 11514979]

Takesian AE, Kotak VC, Sanes DH. Presynaptic GABA(B) receptors regulate experience-dependent development of inhibitory short-term plasticity. J Neurosci. 2010; 30:2716–2727. [PubMed: 20164356]

Takesian AE, Kotak VC, Sharma N, Sanes DH. Hearing loss differentially affects thalamic drive to two cortical interneuron subtypes. J Neurophysiol. 2013; 110:999–1008. [PubMed: 23719211]

Tao HW, Poo MM. Activity-dependent matching of excitatory and inhibitory inputs during refinement of visual receptive fields. Neuron. 2005; 45:829–836. [PubMed: 15797545]

Tropea D, Majewska AK, Garcia R, Sur M. Structural dynamics of synapses in vivo correlate with functional changes during experience-dependent plasticity in visual cortex. J Neurosci. 2010; 30:11086–11095. [PubMed: 20720116]

van Versendaal D, Rajendran R, Saiepour MH, Klooster J, Smit-Rigter L, Sommeijer JP, De Zeeuw CI, Hofer SB, Heimel JA, Levelt CN. Elimination of inhibitory synapses is a major component of adult ocular dominance plasticity. Neuron. 2012; 74:374–383. [PubMed: 22542189]

Wilson NR, Runyan CA, Wang FL, Sur M. Division and subtraction by distinct cortical inhibitory networks in vivo. Nature. 2012; 488:343–348. [PubMed: 22878717]

Wolff SB, Grundemann J, Tovote P, Krabbe S, Jacobson GA, Muller C, Herry C, Ehrlich I, Friedrich RW, Letzkus JJ, et al. Amygdala interneuron subtypes control fear learning through disinhibition. Nature. 2014; 509:453–458. [PubMed: 24814341]

Wu GY, Cline HT. Stabilization of dendritic arbor structure in vivo by CaMKII. Science. 1998; 279:222–226. [PubMed: 9422694]

Xu H, Khakhalin AS, Nurmikko AV, Aizenman CD. Visual experience-dependent maturation of correlated neuronal activity patterns in a developing visual system. J Neurosci. 2011; 31:8025–8036. [PubMed: 21632924]

Xue M, Atallah BV, Scanziani M. Equalizing excitation-inhibition ratios across visual cortical neurons. Nature. 2014; 511:596–600. [PubMed: 25043046]

Zhou M, Liang F, Xiong XR, Li L, Li H, Xiao Z, Tao HW, Zhang LI. Scaling down of balanced excitation and inhibition by active behavioral states in auditory cortex. Nat Neurosci. 2014; 17:841–850. [PubMed: 24747575]

Highlights

- Experience-dependent plasticity identifies 2 groups of inhibitory neurons
- The 2 groups display opposite bimodal plasticity to dark and visual experience
- Experience potentiates visually-evoked E and I inputs and E/I is maintained
- Functionally antagonist inhibitory neurons maintain stability in nascent circuits

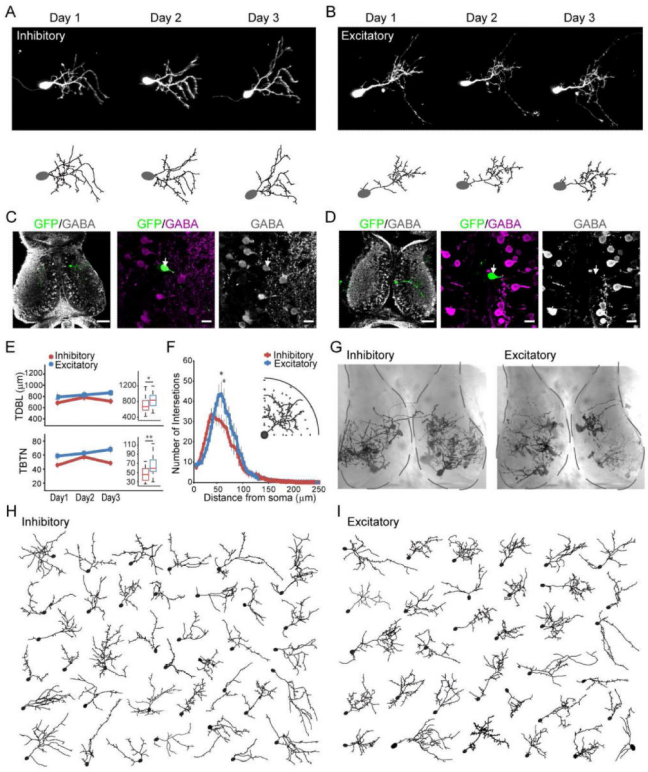

Figure 1.

Inhibitory and excitatory tectal neurons have similar dendritic arbor morphology. A.B. Daily time-lapse images (top) and complete dendritic reconstructions (bottom) of inhibitory (A) and excitatory (B) neurons for each time point. C.D. GABA immunolabeling was used to identify inhibitory and excitatory GFP+ imaged neurons. Left panels: low mag maximum projections of the GFP+ neuron (green) immunostained for GABA (gray). Scale bar: 50μm. Middle and right panels: Single optical sections of the GFP neuron and GABA immunolabeling. Arrows mark locations of the soma. Scale bar: 10 μm. E. No change in TBTN and TDBL in excitatory and inhibitory neurons over the 3-day imaging period (inhibitory neurons, n=16; excitatory neurons, n=14, $p>0.05$, Kruskal-Wallis test). Inset: boxplots of TDBL and TBTN of excitatory and inhibitory neurons on day 3. Boxes show 25^{th} and 75^{th} percentiles and whiskers show 95^{th} percentiles. * $p< 0.05$. Mann-Whitney U test. F. Sholl analysis of dendritic arbor branching patterns of excitatory and inhibitory neurons from day 3 data (panel E). Inset: Illustration of Sholl analysis. Data binned every 5μm, * $p< 0.05$, Mann-Whitney U test. G. Locations of imaged neurons in tectum shown by superimposing live images of individual neurons on a DIC image of the tectum. Tecta are outlined in dashed lines. H. I. Reconstructed dendritic arbors of inhibitory (H) and excitatory (I) neurons, oriented to rostral, caudal, medial and lateral axes of the tectum.

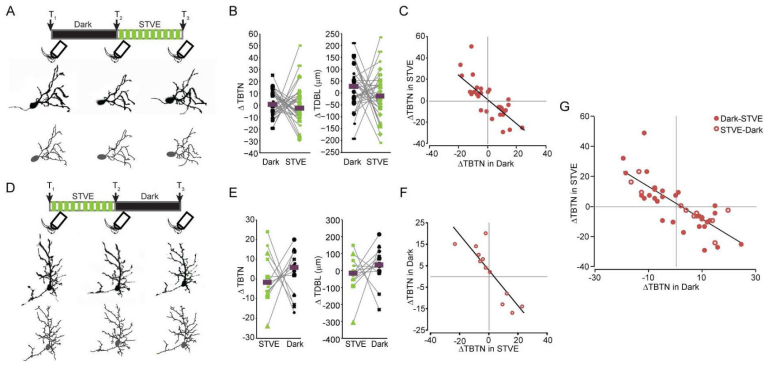

Figure 2.

Inhibitory tectal neurons show bimodal structural plasticity in response to visual experience. A, D. Top: Schematics of visual experience protocols and imaging time points. Bottom: Projected negative images (upper row) and dendritic arbor reconstructions (lower row) of a representative neuron imaged at T_1, T_2 and T_3. B, E. Changes in TBTN (left) and TDBL (right) in response to dark and STVE. Medians are marked by magenta bars. Data from the individual neurons are linked by lines here and in subsequent figures. $p>0.05$, Wilcoxon sign rank test. C, F. Scatterplots of changes in TBTN in response to STVE versus dark (C) or dark versus STVE (F) in individual neurons. G. Overlay of the datasets from the dark/STVE and STVE/dark paradigms, both plotted as changes in STVE versus changes in dark. Dark/STVE: n=30; STVE/Dark: n=12.

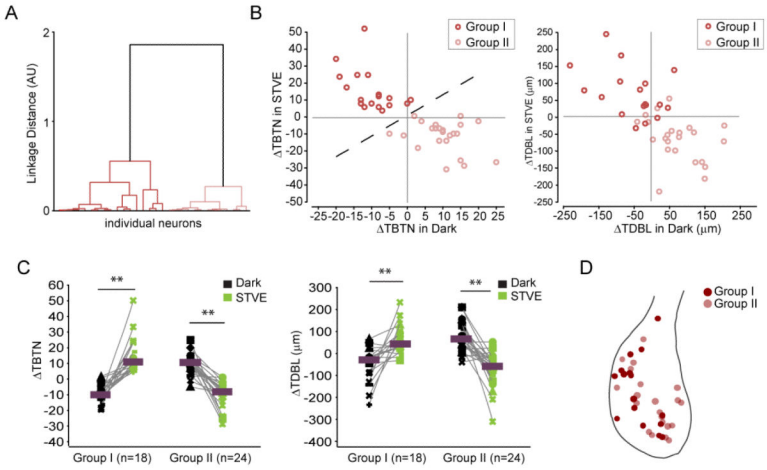

Figure 3.

Cluster analysis of experience-dependent structural changes distinguishes two populations of inhibitory neurons. A. Dendrogram of unsupervised hierarchical cluster analysis based on changes in TBTN in STVE versus dark. B. Scatterplots of changes in TBTN (left) and TDBL (right) in response to STVE versus dark in individual neurons for Group I and Group II inhibitory neurons. C. Changes in TBTN and TDBL in dark and STVE for Group I and Group II inhibitory neurons. Magenta bars mark medians. Group I, n=18; Group II, n=24. **: $p<0.01$, Wilcoxon sign rank test. D. Tectal locations of Group I and Group II somata.

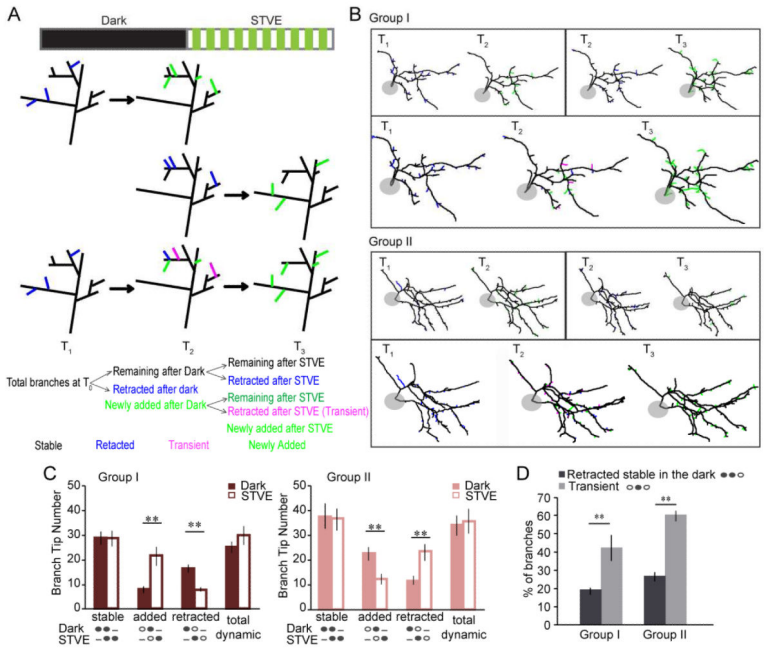

Figure 4.

Different experience-dependent branch dynamics in Group I and Group II inhibitory neurons. A. Schematic of branch dynamics analysis. Top two rows: paired comparison of adjacent time points (T_1 versus T_2; T_2 versus. T_3). Bottom row: serial analysis based on results of the paired comparison. Color scheme: black (stable branches), blue (retracted branches), green (newly added branches), magenta (transient branches). B. Images of dynamic analysis of Group I and Group II inhibitory neurons. Top panels: paired analysis (T_1 versus T_2; T_2 versus T_3). Bottom panels: serial analysis. Color scheme as in A. C. Branch tip numbers in each dynamic category for Group I (red) and II (pink) in response to dark or STVE. Schematics under the bars illustrate the status of the branch at each imaging time point. Solid oval: present. Empty oval: not present. Dash: not relevant. D. Breakdown of branches retracted in STVE based on their history. *: $p<0.05$; **: $p<0.01$, Wilcoxon sign rank test. Data presented as mean±SEM.

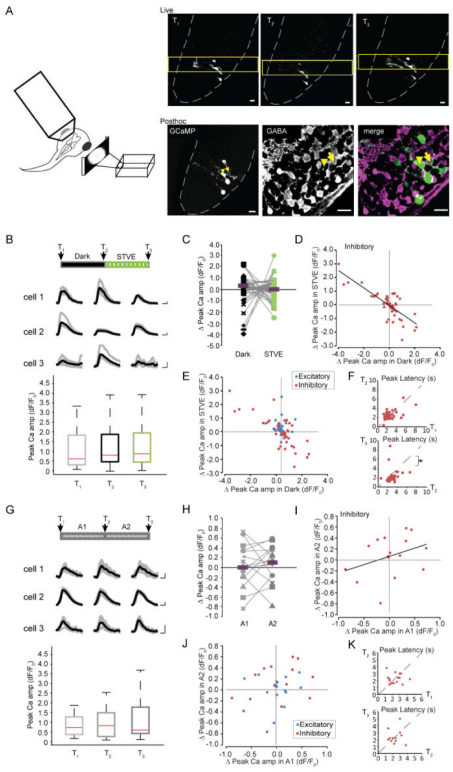

Figure 5.

Bimodal visual experience-dependent functional plasticity in inhibitory neurons. A. Left: illustration of experimental set up for calcium imaging. Right top: Live images at T_1, T_2 and T_3. Yellow frame marks the clip imaged for time series. Gray dashed lines outline the tectum. Right bottom: Posthoc analysis of GABA-immunoreactivity in GCaMP6-expressing neurons. GCaMP fluorescence in the fixed tissue (low-mag single optic section, left) shows somata location of the imaged cells as seen in the live image. GABA immunoreactivity (middle) and merge of GABA immunoreactivity and GCaMP (right). Yellow arrowhead marks a GABA-negative excitatory cell. Yellow arrow marks a GABA-positive inhibitory neuron. Scale bars: 10μm. B. Boxplots of peak amplitude of visually-evoked Ca^{++} responses from all inhibitory neurons (n=49) at T_1, T_2 and T_3 during the Dark/STVE protocol. Inset: Visually-evoked Ca^{++} responses of individual inhibitory neurons. Gray: Overlay of traces from five single trials per cell per time point; Black: averaged traces. Scale bar: 2 sec, 100% dF/F_0. C. Changes in Ca^{++} amplitude in response to dark and STVE, respectively. Magenta bars mark the medians. D. Scatterplots of individual changes in Ca^{++} response amplitude (STVE versus Dark). E. Overlay of scatterplots for individual inhibitory and excitatory neurons shows the different variance of changes after dark and STVE in the two neuron populations. F. Scatterplots of peak latency of Ca^{++} response at T_2 versus T_1 and T_3 versus T_2 in inhibitory neurons show a significant decrease in peak latency after STVE. *: $p<0.05$, Wilcoxon sign rank test. G. Peak amplitude of visually-evoked Ca^{++} responses in inhibitory neurons (n=16) at T_1, T_2 and T_3 in the A_1-A_2 paradigm. Inset: representative Ca^{++} transients from individual inhibitory neurons. H. Changes in Ca^{++} peak amplitude in inhibitory neurons during A_1 and A_2. I. Scatterplots of individual changes in Ca^{++} response (A_2 versus A_1, note difference in the scale compared to D). J. Overlay of inhibitory and excitatory

scatterplots shows no difference in the variance of changes in the two populations. K. Scatterplots of peak latency of Ca^{++} response at T_2 versus T_1 and T_3 versus T_2 in inhibitory neurons show no change in peak latency following A_1 or A_2.

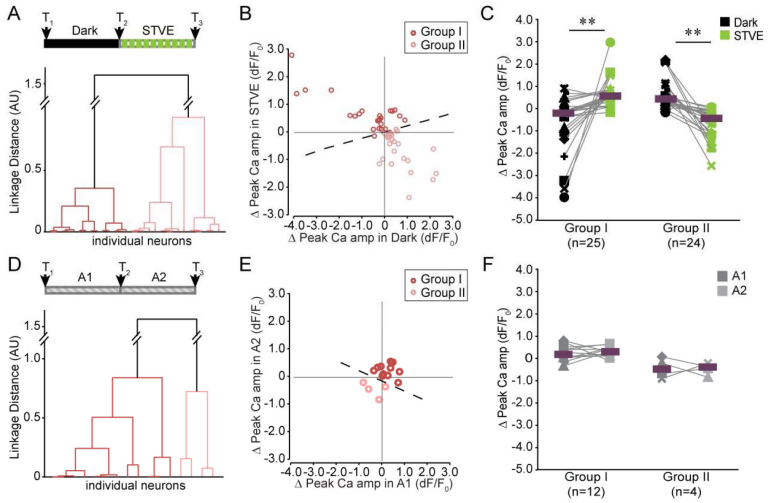

Figure 6.

Cluster analysis of experience-dependent changes in visually-evoked Ca^{++} responses of individual neurons revealed two groups of inhibitory neurons. A. Dendrogram of unsupervised hierarchical clustering based on individual changes in Ca^{++} amplitudes in dark-STVE paradigm. The two groups are shown in red and pink. B. Scatterplot of changes in individual neuronal responses in Group I and Group II neurons. C. Changes in peak Ca^{++} responses over dark or STVE for Group I (n=25) and Group II (n=24) inhibitory neurons. **: $p<0.01$, Wilcoxon sign rank test. Magenta bars mark the medians D. Dendrogram of unsupervised hierarchical clustering based on changes in Ca^{++} response amplitudes in A_1-A_2 paradigm. E. Scatterplot of changes in individual Ca^{++} responses in Group I (n=12) and Group II (n=4). F. Changes in peak Ca^{++} responses over A_1 and A_2 for Group I and Group II neurons.

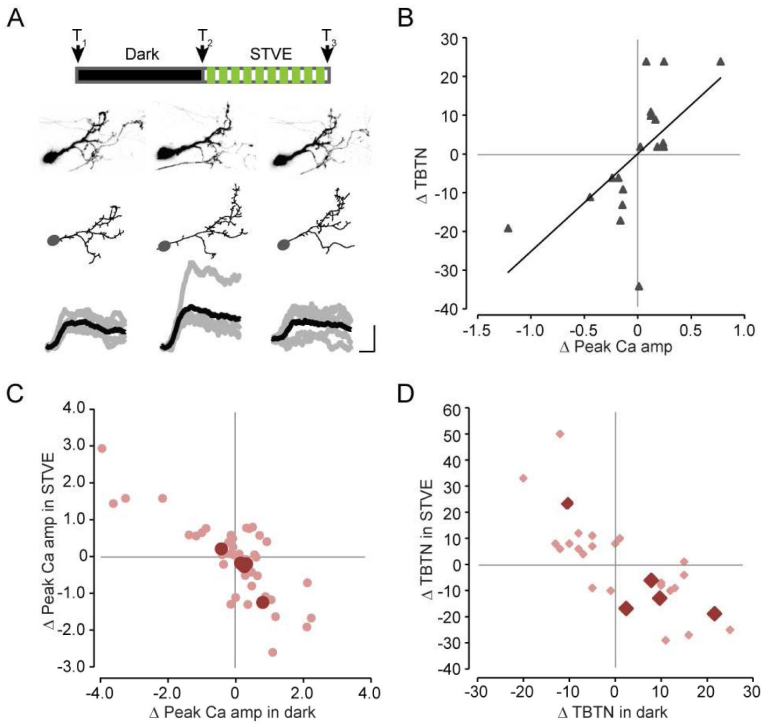

Figure 7.

Experience-dependent dendritic arbor structural plasticity and functional plasticity are correlated in individual neurons. A. Top: Schematic of visual stimulation protocol and imaging time points. Bottom: Projected images (upper row) and reconstructions (middle row) of the complete dendritic arbor and visually-evoked Ca^{++} responses (bottom row) of a tectal neuron at T_1, T_2 and T_3. Scale bar: 2 sec, 10% dF/F_0. B. Scatterplot of changes in total branch tip number (TBTN) versus changes in peak Ca^{++} amplitude (dF/F_0) in response to either dark or STVE in individual neurons (n=10 neurons, 18 data points). r = 0.584, $p<0.05$, Pearson correlation. C, D. Scatterplots overlaying changes of peak Ca^{++} amplitude (C) and TBTN (D) of individual inhibitory neurons shown in B (dark pink, n=5) onto the entire datasets presented in previous figures (light pink).

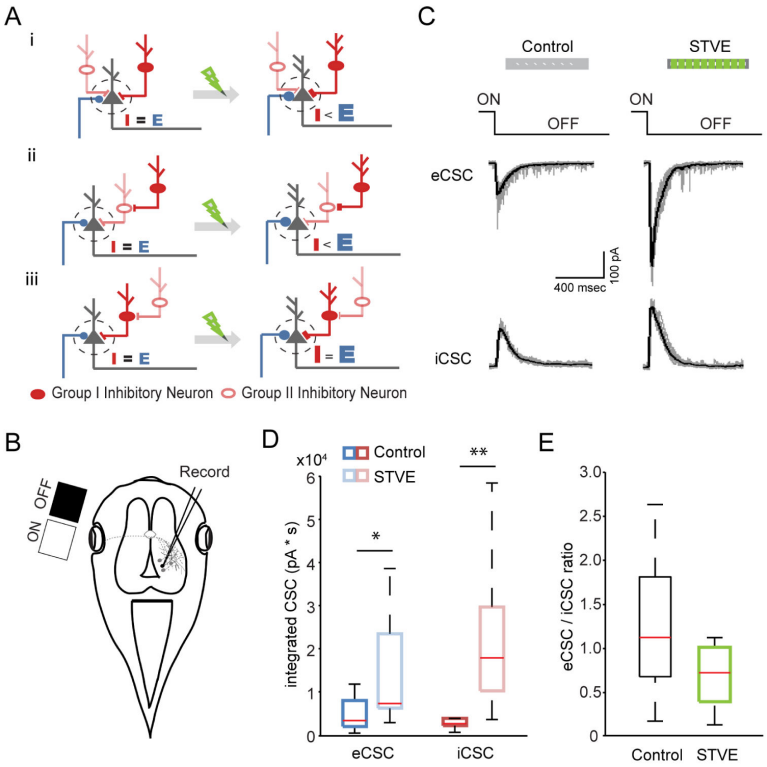

Figure 8.

E/I is maintained after visual experience. A. Three cartoons of circuit connectivity diagrams (i, ii, iii) showing the effect of visual experience on E/I balance in postsynaptic neurons. See text for details. B. Schematic of experimental set up of the in vivo electrophysiological recording of visually-evoked postsynaptic responses in tectal neurons. C. Representative whole cell excitatory and inhibitory compound synaptic currents recorded at −60 mV and 0mV, respectively, in response to light-off stimuli. Scale bar: 400msec, 100pA. D. Boxplots of total integrated excitatory and inhibitory compound synaptic currents evoked by visual stimulation in animals after 4hr of ambient light (control) or STVE. n=10 cells for each group, *: $p<0.05$, **: $p<0.01$, Mann-Whitney U test. E. Boxplots of eCSC/iCSC. $p>0.05$, Mann-Whitney U test.